Allosteric Control of Acetylcholinesterase Activity by Monoclonal Antibodies

Ashima Saxena,* Regina Hur, and B. P. Doctor

Division of Biochemistry, Walter Reed Army Institute of Research, Washington, DC 20307-5100

Received August 19, 1997; Revised Manuscript Received October 28, 1997[⊗]

ABSTRACT: Previous studies showed that monoclonal antibodies raised against phosphorylated fetal bovine serum acetylcholinesterase appeared to modulate the catalytic activity of the enzyme by binding to a conformational epitope located at or near the region of the peripheral anionic site. The mechanism of inhibition of acetylcholinesterase by these monoclonal antibodies was further investigated by determining their effect on (i) substrate inhibition due to the binding of excess substrate to the peripheral anionic site and (ii) binding of peripheral anionic site ligands, such as propidium and fasciculin. Results of these experiments demonstrate that the accessibility of substrate to the peripheral anionic site in these complexes was restricted but not completely blocked, as none of the monoclonal antibodies eliminated the phenomenon of excess substrate inhibition. The results also show that propidium clearly slowed the inhibition of fetal bovine serum acetylcholinesterase by all six inhibitory monoclonal antibodies but to different levels. Complexation of fetal bovine serum acetylcholinesterase with monoclonal antibodies 25B1, 4E5, 6H9, and 5E8 interfered with the binding of fasciculin to the complexed enzyme, suggesting that part of their epitope overlapped with the fasciculin binding site. These monoclonal antibodies bind, in part, at the peripheral anionic site, since polyclonal anti-idiotypic antibodies generated against two monoclonal antibodies, 25B1 and 6H9, bound stoichiometric amounts of propidium. Like fasciculin, binding of these monoclonal antibodies in the vicinity of the peripheral anionic site at the rim of the active site gorge allosterically affects the orientation of W86 located at the base of the gorge, resulting in inhibition of enzyme activity.

Acetylcholinesterase (AChE; EC 3.1.1.7)[1] is a serine hydrolase that causes the termination of neuronal transmission at the cholinergic synapse by hydrolyzing its natural substrate, acetylcholine (*1*). The catalytic center of the enzyme is composed of an 'esteratic' subsite and an 'anionic' subsite (*2*). In addition to the active site, a 'peripheral' anionic site remote from the active site on the surface of the molecule has also been identified (*3*). These sites were distinguished by enzyme kinetic and ligand binding studies using edrophonium, which binds specifically to the active site, and propidium, which binds primarily to the peripheral anionic site (*3*). On the other hand, bisquaternary ligands such as decamethonium can span the two anionic sites which are ≈14 Å apart (*4*). The X-ray crystal structure of *Torpedo* AChE shows that the active site of the enzyme, composed of a catalytic triad formed by residues S200, H440, and E327, is located at the base of a deep and narrow gorge lined primarily with aromatic amino acid residues (*5*). Evidence from structural and chemical data suggests that residues W84 and F330 belong to the anionic subsite located in the active site gorge and W279, Y121, and Y70 to the peripheral anionic site located at the entrance of the gorge (*5*−*9*).

We recently reported the production and characterization of six inhibitory monoclonal antibodies (MAbs) against natural or modified forms of fetal bovine serum (FBS) AChE (*10*). These MAbs were prepared to map the topography of the surface of the enzyme molecule and to identify other regions of the molecule which may be involved in its catalytic function. As expected, none of these MAbs bound to the active site of the enzyme, which is located deep inside the gorge and is not accessible to the MAbs. These MAbs appeared to modulate the catalytic activity of FBS AChE by binding to a conformational epitope located on the surface at or near the region of the peripheral anionic site (*10*).

The binding of MAbs can cause inhibition of enzyme activity by several possible mechanisms, two of which include steric occlusion of substrate entry into the active site gorge and/or an allosteric effect on the active site influencing substrate catalysis. Binding studies of DFP with FBS AChE−MAb complexes revealed that the nucleophilicity of the active site serine of the various complexes had been altered. Although the active site was still accessible for displacement of DFP by TMB_4, the extent of dephosphorylation was different for various FBS AChE−MAb complexes. These results suggest that the entrance to the catalytic site was somewhat restricted in these complexes which could be due to MAb-induced conformational changes in the active site gorge or steric hindrance, or both (*10*). Evidence for

* Corresponding author.

⊗ Abstract published in *Advance ACS Abstracts,* December 15, 1997.

[1] Abbreviations: AChE, acetylcholinesterase; FBS, fetal bovine serum; MAb, monoclonal antibody; IgG, immunoglobulin; ATC, acetylthiocholine; DTNB, 5,5′-dithiobis(2-nitrobenzoic acid); DFP, diisopropyl fluorophosphate; edrophonium, ethyl(*m*-hydroxyphenyl)-dimethylammonium chloride; propidium, 3,8-diamino-5′,3′-(trimethylammonium)propyl-6-phenylphenanthridium iodide; TMB_4, 1,1-trimethylenebis(4-hydroximinomethyl)pyridinium dibromide; MEPQ, 7-(methylethoxyphosphinyloxy)-1-methylquinolinium iodide; IPA, indophenyl acetate.

S0006-2960(97)02061-8
Published on Web 01/06/1998

MAb-induced conformational changes in the active site gorge was provided by electron paramagnetic resonance studies with the FBS AChE−Fab 25B1 complex (*11*).

In this study, we have analyzed the mechanism of inhibition of AChE by these MAbs in detail by studying their effect on peripheral anionic-site function of the enzyme. The results presented here show that these MAbs bind at differing but overlapping epitopes located in the vicinity of the peripheral anionic site of the enzyme molecule and can be classified into two groups. The first group includes MAbs 4E5, 25B1, and 13D8 which, upon complexation with FBS AChE, did not interfere with binding of substrate to the active site and the peripheral anionic site. The second group includes MAbs 5E8, 6H9, and 2A1 which, upon binding to FBS AChE, affected the binding of substrate to the active site as well as the peripheral anionic site. MAbs 4E5, 25B1, 5E8, and 6H9 interfered with the binding of fasciculin to these complexes, suggesting that part of their epitope overlapped with the fasciculin binding site on AChE. The binding of these MAbs in the vicinity of the peripheral anionic site allosterically affects the orientation of W86(*84*)[2] which stabilizes the quaternary group of the substrate, resulting in inhibition of enzyme activity. We also used the anti-idiotypic antibody approach to identify the MAb combining site. Polyclonal anti-idiotypic antisera were raised in rabbits against two of these MAbs, 25B1 and 6H9. Both anti-idiotypic antibodies bound propidium in stoichiometric amounts, indicating that these anti-idiotypic antibodies displayed internal image properties of the original immunogen, the FBS AChE peripheral anionic site. The lower dissociation constant of anti-6H9 (K_D = 0.12 μM) for propidium compared to anti-25B1 (K_D = 2.5 μM) also supports the notion that although both MAbs 25B1 and 6H9 bind in the vicinity of the peripheral anionic site, the epitopes are slightly different.

EXPERIMENTAL PROCEDURES

Materials. ATC, DTNB, edrophonium and propidium were obtained from Sigma Chemical Co. (St. Louis, MO). The procedure for the production and purification of MAbs has been previously described (*10*). Fab fragments of MAbs were prepared and purified using the Immunopure Fab preparation kit from Pierce (Rockford, IL). Polyclonal anti-idiotypic antibodies to these Fab fragments were produced by hyperimmunizing rabbits with Fab fragments suspended in 0.9% saline. Electrophoretically pure AChE from FBS was purified as described (*13*). Purified fasciculin 2 isolated from *Dendroaspis angusticeps* venom was obtained (in lyophilized form) from Alomone Labs (Jerusalem, Israel). Fasciculin 2 was resuspended in 50 mM sodium phosphate, pH 8.0, containing 0.05% BSA, and the concentration of fasciculin in solution was determined spectrophotometrically at λ_{max} = 276 nm (ϵ = 4900 M^{-1} cm^{-1}).

Measurement of AChE Activity. AChE activity was measured in 50 mM sodium phosphate, pH 8.0, at 25 °C, using ATC as the substrate (*14*). Substrate inhibition was investigated by measuring the enzyme activity of FBS AChE and various FBS AChE−MAb complexes over a substrate concentration range of 0.05−20 mM. The kinetic constants for the hydrolysis of ATC were determined by analyzing the data according to the Haldane equation (*15*):

$$v = \frac{V_{max}}{1 + [S]/K_{SS} + K_m/[S]} \quad (1)$$

where K_m is the Michaelis−Menten constant and K_{SS} is a substrate inhibition constant representing dissociation of a second substrate molecule.

Kinetics of FBS AChE Inhibition by MAbs. Each MAb at a concentration varying from 0.1 to 15 μM was diluted into FBS AChE (∼1.0 nM active site) in 1 mL of 5 mM sodium phosphate, pH 8.0, containing 0.01% BSA at 25 °C. Residual enzyme activity was measured at 2 min intervals by assaying 100 μL of the reaction mixture using the Ellman assay (*14*). The effect of edrophonium or propidium on the rate of the inhibition reaction was determined by incubating FBS AChE with 1 μM edrophonium or 3.35 μM propidium for 5 min prior to the addition of MAb. The time course of inhibition reactions was analyzed using a nonlinear fit of the data to the equation:

$$AChE_t = (AChE_0 - AChE_f)e^{-kt} + AChE_f \quad (2)$$

where $AChE_t$ is the enzyme activity at time t, $AChE_0$ is the activity at time t = 0, $AChE_f$ is the final residual activity, and k is the pseudo-first-order rate constant for the association reaction. The second-order rate constant k_{on}, was obtained by dividing k by the concentration of MAb.

Preparation of FBS AChE−MAb Complexes. For the preparation of FBS AChE−MAb complexes, 25 pmol of FBS AChE was used, and the amount of MAb was varied to yield AChE−MAb molar ratios of 1 to 5. The complexes were incubated overnight at 22 °C, and residual enzyme activity was measured by the Ellman assay (*14*).

Inhibition of Enzyme Activity by Fasciculin 2. The interaction of fasciculin and substrate with AChE can be described by Scheme 1, where the substrate interacts at the active site as well as the peripheral anionic site, and fasciculin interacts only at the peripheral anionic site (*16*).

In Scheme 1, F, S, and E represent free fasciculin, substrate, and enzyme, ES is the enzyme−substrate complex, and FE and SE are peripheral site complexes with fasciculin and substrate, respectively. The ratio k_{-F}/k_F is equal to K_i, the reversible inhibition constant for the inhibition of enzyme

Scheme 1

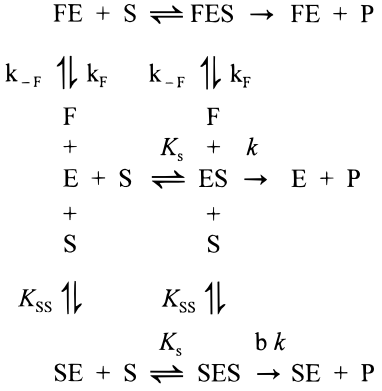

[2] The dual numbering system gives the residue number in human AChE followed by the corresponding residue in *Torpedo* AChE (*12*).

by fasciculin. Aliquots of enzyme alone (0.5 nM) or complexed with various MAbs were mixed with increasing concentrations of fasciculin (0−20 nM) and incubated overnight at 22 °C. Samples were assayed for residual enzyme activity (*14*), and the data were analyzed according to the following equations derived from Scheme 1 (*16*):

$$v_{i\beta} = v_i[1 + \beta[\mathrm{F}]/(K_i + v_i/k)] \qquad (3)$$

where v_i is described as (*17*)

$$v_i = k\{([\mathrm{E}] - K_i - [\mathrm{F}]) + [(K_i + [\mathrm{F}] + [\mathrm{E}])^2 - 4[\mathrm{F}][\mathrm{E}]]^{1/2}\}/2$$

with the constraints of $K_m << S << K_{SS}$ and [F] ≅ [E].

Determination of Affinity Constants for the Binding of MAbs to FBS AChE. The interaction of MAbs with FBS AChE is similar to that described for fasciculin. Aliquots of enzyme (0.5 nM) were mixed with increasing concentrations of MAbs (0−200 nM) depending on the MAb and incubated overnight at 22 °C. Samples were assayed for residual enzyme activity (*14*), and the affinity constants for binding of MAbs to FBS AChE were calculated by analyzing the data according to eq 3 as described above.

Purification of IgG Fractions Containing Polyclonal Anti-idiotypic Antibodies. The rabbit polyclonal anti-idiotypic antibodies to either 25B1 or 6H9 were precipitated using ammonium sulfate (0−35% saturation). The pellets after centrifugation were dissolved in 50 mM sodium phosphate, pH 8.0, and dialyzed against the same buffer. IgG-enriched fractions were obtained by affinity chromatography on protein A−Sepharose using the Immunopure IgG1 purification kit from Pierce (Rockford, IL). The anti-idiotypic antibodies were expected to comprise 5−10% of the total IgG present in these antisera and were used without further purification.

Assay for Polyclonal Anti-idiotypic Antibodies. The presence of anti-idiotypic antibodies in the sera of rabbits immunized with MAbs 25B1 and 6H9 was detected by a competitive enzyme inhibition assay. Four sets of tubes containing either 0−5 pmol of 25B1 or 0−10 pmol of 6H9 were set up. To the first set of tubes was added 100 μL of buffer (50 mM sodium phosphate, pH 8.0, containing 0.01% BSA); to the second set of tubes was added 100 μL of buffer containing 500 pmol of preimmune IgG; to the third set of tubes was added 100 μL of buffer containing 100 pmol of IgG containing anti-idiotypic antibodies; to the fourth set of tubes was added 100 μL of buffer containing 300 pmol of IgG containing anti-idiotypic antibodies. The mixtures were incubated overnight at 4 °C. One unit (2.5 pmol) of FBS AChE was added to each tube and incubated for 4 h at 22 °C. The enzyme activity in each tube was determined by the Ellman assay (*14*).

Fluorescence Titrations. Fluorescence titrations of IgG fractions containing polyclonal anti-idiotypic antibodies with propidium were carried out using a Perkin Elmer MPF-66 fluorescence spectrophotometer. The fluorometer was equipped with a thermostated 4-cell turret so that a sample and a buffer blank could be titrated at the same time. Two microliter aliquots of propidium, $(1 \times 10^{-6})-(1 \times 10^{-4})$ M in water, were added to 225 μL of anti-idiotypic antibody solution in 5 mM Tris·HCl, pH 8.0. The fluorescence of propidium was measured using an excitation wavelength of 520 nm and an emission wavelength of 625 nm. The measured fluorescence was corrected for changes in excitation energy, inner filter effects, and changes in sample volumes during titration by parallel titrations of buffer blanks. The dissociation constants (K_D) of propidium for the two anti-idiotypic antibodies and FBS AChE were determined by analyzing the data using Scatchard plots. The concentrations of free (P_f) and bound (P_b) propidium were obtained from the equation (*18*):

$$[\mathrm{P_f}] = (I_o - \gamma'[\mathrm{P_o}])/(\gamma - \gamma') \qquad [\mathrm{P_b}] = [\mathrm{P_o}] - [\mathrm{P_f}]$$

where I_o is the observed fluorescence intensity, $[P_o]$ is the concentration of propidium, and γ and γ' are the fluorescence coefficients of free and bound propidium, respectively (*19*).

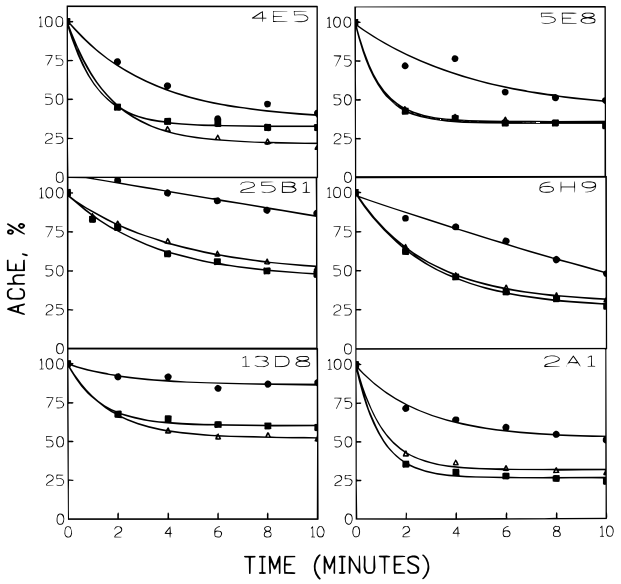

FIGURE 1: Effect of edrophonium and propidium on the rate of inhibition of FBS AChE by various MAbs. Each MAb at a concentration varying from 0.1 to 15 μM was diluted into FBS AChE (0.5−1.0 nM active site) in 5 mM sodium phosphate, pH 8.0, containing 0.01% BSA at 25 °C (final volume of 1 mL). Residual enzyme activity was measured at 2 min intervals by assaying 100 μL of the reaction mixture using the Ellman assay (*14*). Data for the time course of inhibition reactions were analyzed using eq 2 and are shown as (■). The effects of 1 μM edrophonium (△) and 3.35 μM propidium (●) on the rate of the inhibition reaction are also shown. In these plots, % AChE = $(AChE_t/AChE_0) \times 100$.

RESULTS

Inhibition of FBS AChE by MAbs. Previous studies with MAbs 25B1 and 6H9 suggested that these two MAbs modulate the activity of FBS AChE by binding to a site at or near the 'peripheral' anionic site located at the rim of the active site gorge (*10*, *20*). To assess the site of interaction of FBS AChE with the six MAbs, we studied the effect of edrophonium, a specific active site ligand, and propidium, a peripheral anionic site ligand, on the kinetics of binding of MAbs to FBS AChE. Figure 1 shows the effect of edrophonium and propidium on the rate of inhibition of FBS AChE by the six MAbs. The data were analyzed according to eq 2, and the effects of edrophonium and propidium on k_{on}, the association rate constant for the binding of MAb to FBS AChE, are shown in Table 1. It was expected that if a

Table 1: Competition of Ligands with MAbs for Binding to FBS AChE[a]

	$k_{on} \times 10^{-4}$ (M^{-1} min^{-1})					
competing ligand	4E5	25B1	13D8	5E8	6H9	2A1
none	0.40 ± 0.02	0.43 ± 0.06	0.29 ± 0.01	0.31 ± 0.03	0.49 ± 0.03	0.49 ± 0.04
edrophonium	0.29 ± 0.02	0.34 ± 0.06	0.22 ± 0.01	0.30 ± 0.03	0.50 ± 0.03	0.44 ± 0.05
propidium	0.15 ± 0.02	0.03 ± 0.01	0.16 ± 0.05	0.06 ± 0.03	0.07 ± 0.05	0.18 ± 0.03

[a] Values of the pseudo-first-order rate constant, k, for the interaction of MAbs with AChE were determined by analyzing the time course of inhibition reactions using a nonlinear fit of the data to eq 2, in the absence or presence of the indicated ligands shown in Figure 1. The second-order rate constant, k_{on}, was obtained by dividing k by the concentration of MAb.

Table 2: Affinity Constants for the Binding of MAbs to FBS AChE

MAb	K_i (nM)[a]	β
4E5	0.05 ± 0.02	0.17 ± 0.03
25B1	0.06 ± 0.03	0.11 ± 0.07
13D8	50 ± 20	0.28 ± 0.04
5E8	0.007 ± 0.003	0.02 ± 0.01
6H9	0.002 ± 0.001	0.07 ± 0.01
2A1	12 ± 4	0.12 ± 0.04

[a] Inhibition constants were determined by incubating FBS AChE with various amounts of MAbs overnight at 22 °C, measuring residual activity, and fitting the data to eq 3.

MAb competed with a ligand for binding to AChE, the presence of the ligand would slow down the association reaction between the enzyme and MAb. Indeed the results show that propidium clearly decreased the k_{on} for the inhibition of FBS AChE by all six inhibitory MAbs but to different levels. Therefore, it appears that these MAbs compete with propidium for binding to the peripheral anionic site. In contrast, edrophonium did not affect the k_{on} for the inhibition of FBS AChE by MAbs 5E8, 6H9, and 2A1. There was a slight effect of edrophonium (~25%) on the rate of inhibition of FBS AChE by MAbs 4E5, 25B1, and 13D8. These results show that the binding of edrophonium to the active site located at the base of the gorge had little or no effect on the rate of binding of MAbs to the peripheral anionic site of AChE located at the rim of the active site gorge.

Affinity Constants for the Binding of MAbs to FBS AChE. Competition experiments with edrophonium and propidium described above suggested that, like fasciculin, these MAbs were interacting primarily at the peripheral anionic site of FBS AChE. Various concentrations of MAbs were incubated with AChE overnight at 22 °C and assayed for residual activity. The data were analyzed according to eq 3. For each MAb, this analysis yielded K_i, the equilibrium dissociation constant for MAb, and β, the fraction of residual activity reflecting partial productivity of the AChE−MAb complex (*16*). The results described in Table 2 show that, of the six MAbs examined, MAbs 5E8 and 6H9 appeared to be the most potent inhibitors of FBS AChE with apparent K_i values in the picomolar range. Residual activities of the complexes ranged from 2 to 7%, suggesting that the binding of these MAbs at the peripheral anionic site significantly affected the catalytic parameters of the enzyme. MAbs 25B1 and 4E5 were almost 10-fold less potent than 6H9 and 5E8 in inhibiting FBS AChE, and their binding influenced the catalytic parameters of the enzyme to a lesser extent. The other two MAbs, 2A1 and 13D8, had K_i values in the nanomolar range and were the least effective in altering enzyme catalysis.

Table 3: Residual Enzyme Activity (in Percent)[a] for Various FBS AChE−MAb Complexes

AChE:MAb ratio	4E5	25B1	13D8	5E8	6H9	2A1
1:0	100	100	100	100	100	100
1:1	3.3	1.2	60	52	11	22
1:2	1.9	1.1	44	ND	2	15
1:3	1.9	1.1	ND	1.4	2	ND
1:5	ND[b]	ND	23	1.4	ND	12

[a] FBS AChE−MAb complexes were prepared by incubating FBS AChE with the indicated amounts of MAbs overnight at 22 °C. Residual enzyme activity was measured using the Ellman assay as described (*14*). [b] Not determined.

Substrate Inhibition of FBS−MAb Complexes. The peripheral anionic site of AChE has also been identified as the substrate inhibition site (*21*). The binding of substrate at this site allosterically affects conformation at the active site, thus affecting acylation and/or deacylation rates. If the MAbs were indeed binding in the vicinity of the peripheral anionic site, they could completely block or restrict the access of substrate to this site, either eliminating the substrate inhibition phenomenon or causing a shift in substrate curves to the right. Therefore, we determined the accessibility of the peripheral anionic site to substrate in these complexes by measuring catalysis as a function of substrate concentration. The complexes were prepared by mixing FBS AChE with varying amounts of MAbs such that the AChE−MAb ratio was 1:1 to 1:5. The complexes were incubated overnight at 22 °C, and the residual enzyme activity was measured (Table 3). For MAbs 4E5, 25B1, 5E8, and 6H9, a 2−3 fold molar excess of MAb over enzyme concentration resulted in >98% inhibition of enzyme activity. With the other two MAbs, 2A1 and 13D8, maximum inhibition of FBS AChE was only 78−90%, even at FBS AChE−MAb ratios of 1:5. The presence of residual AChE activity in the presence of a molar excess of MAb suggests that the active site in these complexes was still accessible to the substrate.

The extent of inhibition in the presence of excess substrate was compared by measuring the enzyme activity of FBS AChE and FBS AChE−MAb complexes using ATC as the substrate in a concentration range of 0.5−20 mM. As shown in Figure 2, FBS AChE clearly displayed excess substrate inhibition beginning at an ATC concentration of ~3 mM. The substrate curves for the complexes of MAbs 4E5 and 13D8 were similar to the substrate concentration curve for free enzyme. Analysis of data using the Haldane equation (eq 1) yielded values for K_m, the Michaelis−Menten constant representing the hydrolysis of substrate at the active site, and K_{SS}, a substrate inhibition constant representing the dissociation of a substrate molecule at the peripheral anionic site (Table 4). The values for K_{SS} were essentially unaffected by complexation of FBS AChE with these MAbs, suggesting

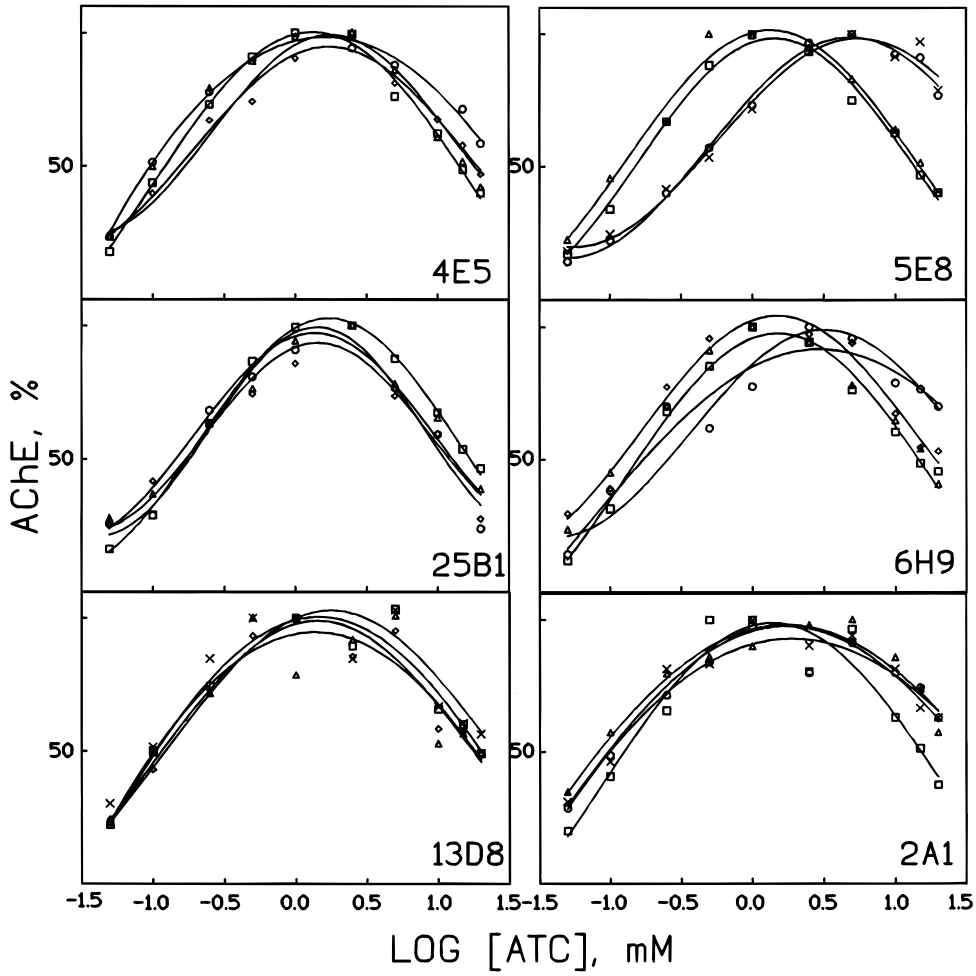

FIGURE 2: Dependence of catalytic activity on ATC concentration for various FBS AChE−MAb complexes. For the preparation of FBS AChE−MAb complexes, 25 pmol of FBS AChE was used, and the amount of antibody was varied to yield AChE:MAb molar ratios of 1 to 5. The complexes were incubated overnight at room temperature, and enzyme activity was measured by the Ellman assay in 50 mM sodium phosphate, pH 8.0 (*14*). The symbols represent FBS AChE:MAb ratios of 1:1 (△), 1:2 (◇), 1:3 (○), and 1:5 (×). FBS AChE control is represented by (□).

Table 4: Kinetic Parameters[a] (mM) for Various FBS AChE−MAb Complexes

AChE:MAb ratio	4E5		25B1		13D8		5E8		6H9		2A1	
	K_m	K_{SS}	K_m	K_{SS}	K_m	K_{SS}	K_m	K_{SS}	K_m	K_{SS}	K_m	K_{SS}
1:0	0.18 ± 0.03	11 ± 2	0.18 ± 0.04	11 ± 2	0.17 ± 0.46	14 ± 4	0.20 ± 0.04	11 ± 2	0.18 ± 0.07	11 ± 5	0.21 ± 0.07	10 ± 3
1:1	0.20 ± 0.07	12 ± 4	0.14 ± 0.05	10 ± 4	0.12 ± 0.04	17 ± 5	0.13 ± 0.05	10 ± 4	0.15 ± 0.02	13 ± 1	0.10 ± 0.02	28 ± 6
1:2	0.14 ± 0.03	16 ± 3	0.4 ± 0.3	5 ± 3	0.17 ± 0.04	12 ± 3	ND	ND	0.25 ± 0.08	68 ± 49	ND	ND
1:3	0.20 ± 0.04	15 ± 3	0.5 ± 0.3	4 ± 2	ND	ND	0.42 ± 0.05	51 ± 11	0.49 ± 0.14	71 ± 13	0.14 ± 0.01	26 ± 3
1:5	ND[b]	ND	ND	ND	0.18 ± 0.08	17 ± 7	0.6 ± 0.2	71 ± 12	ND	ND	0.12 ± 0.02	25 ± 5

[a] Kinetic constants were determined by measuring activity versus ATC concentration and fitting the data to eq 1. [b] Not determined.

that the accessibility of substrate to the peripheral anionic site was unaffected by the binding of MAbs to this site. For the complex of MAb 25B1, there was >60% reduction in K_{SS} compared to free enzyme. However, for complexes of MAbs 6H9, 5E8, and 2A1, the substrate curves were displaced to the right, suggesting that these MAbs interfered with the binding of substrate to the peripheral anionic site of FBS AChE. This was reflected by increasing K_{SS} values with increasing MAb concentrations in these complexes (Table 4). These results also demonstrate that the accessibility of substrate to the peripheral anionic site in these complexes is restricted but not completely blocked, as none of the MAbs eliminated the phenomenon of excess substrate inhibition, a characteristic unique to AChEs. The displacement of substrate curves to the right for complexes with MAbs 6H9, 5E8, and 2A1, compared to the curve for free enzyme, suggests that these MAbs bind to AChE and affect its activity slightly differently from MAbs 4E5, 25B1, and 13D8.

All FBS AChE−MAb complexes retained some residual activity even in the presence of excess MAbs, indicating that enzyme acylation as well as deacylation still occurred when MAbs were bound to the enzyme. The first-order rate constant for enzyme acylation and deacylation, k_{cat} ($V_{max} = k_{cat}[E_{tot}]$), for complexes of FBS AChE with MAbs 25B1, 6H9, 4E5, and 5E8, was ∼1−3% of the k_{cat} value for free enzyme (Table 3; since $[E_{tot}] = 25$ pmol in all these complexes, $V_{max} = k_{cat} \times$ constant). The second-order rate constants, k_{cat}/K_m, in the presence of these MAbs were 0.4−1% of the corresponding values in the absence of MAbs

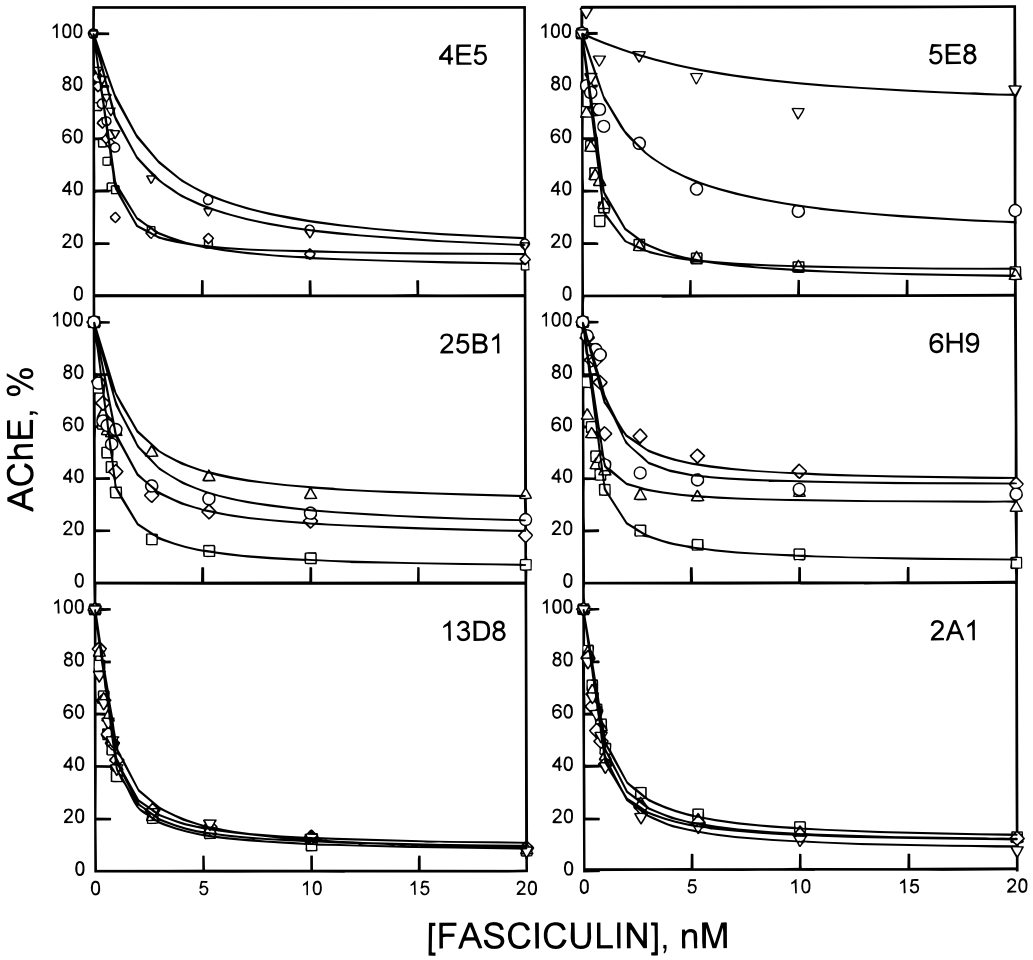

FIGURE 3: Effect of fasciculin 2 on the residual activity of FBS AChE−MAb complexes. For the preparation of FBS AChE−MAb complexes, 25 pmol of FBS AChE was used, and the amount of MAb was varied to yield FBS AChE:MAb molar ratios of 1 to 5. Aliquots of each complex containing 0.5 nM FBS AChE were incubated with fasciculin (0−20 nM) overnight at 22 °C, and enzyme activity was measured by the Ellman assay in 50 mM sodium phosphate, pH 8.0 (*14*). The symbols represent complexes with FBS AChE−MAb molar ratios of 1:1 (△), 1:2 (◇), 1:3 (○), and 1:5 (▽). FBS AChE control is represented by (□).

(Tables 3 and 4). Since the first- and second-order rate constants for ATC hydrolysis decreased to nearly the same extent and the K_m values of these complexes were within 3-fold of the K_m values for the free enzyme, it appears that these MAbs are predominantly noncompetitive inhibitors of AChE. As the active site of AChE is located in a deep, narrow gorge which is inaccessible to large antibody molecules, these results suggest that binding of MAbs at the peripheral anionic site allosterically controlled the hydrolysis of substrate by the enzyme.

Fasciculin 2 Binding to FBS AChE−MAb Complexes. The peripheral anionic site of AChE is also the site of interaction of fasciculin, a peptide toxin found in the venom of snakes of the mamba family (*22*−*24*). Site-directed mutagenesis studies and the X-ray crystal structure of the AChE−fasciculin complex showed that binding of fasciculin involves the aromatic residues W286(*279*), Y72(*70*), and Y124(*121*), located at the rim of the gorge (*24*−*26*). In order to determine if fasciculin and the MAbs shared the same binding site on the surface of AChE, the accessibility of the peripheral anionic site to fasciculin in these complexes was determined by measuring residual enzyme activity as a function of fasciculin concentration, shown in Figure 3. The starting residual activity was ∼2% of the original activity for complexes with MAbs 25B1, 6H9, 4E5, and 5E8 and ∼20% for complexes with 2A1 and 13D8.

The interaction of fasciculin 2 with AChE shown in Scheme 1 can be defined by two parameters that represent two processes: the first process, defined by K_i, represents the binding of fasciculin to the aromatic residues at the rim of the gorge; and the second process, defined by β, represents the allosteric effect of this interaction on the active site located at the base of the gorge (*16*). A nonlinear fit of the data to eq 3 yielded K_i, the dissociation constant for fasciculin, and β, the fraction of residual activity (*16*). Therefore, competition between fasciculin and MAbs for binding to the peripheral anionic site would be reflected by changes in K_i or β, or both. The results of this study show that fasciculin inhibited FBS AChE at subnanomolar concentrations (Table 5). Since MAbs 25B1, 6H9, 4E5, and 5E8 have a higher affinity for FBS AChE (Table 2) compared to fasciculin (Table 5), fasciculin would not be able to displace the MAbs if they occupied its binding site on the enzyme molecule. Complexes of FBS AChE with MAbs 6H9 and 5E8 at saturating concentrations of MAb showed the highest residual enzyme activity (38−75%) and altered the dissociation constant, K_i, for fasciculin. Complexes of FBS AChE with MAbs 4E5 and 25B1 at saturating concentrations of MAb showed residual activities of 15−30% with

Table 5: Inhibition Constants[a] (nM) for Fasciculin 2 with Various FBS AChE−MAb Complexes

AChE:MAb ratio	4E5		25B1		13D8		5E8		6H9		2A1	
	K_i	β	K_i	β	K_i	β	K_i	β	K_i	β	K_i	β
1:0	0.5 ± 0.1	0.1 ± 0.01	0.4 ± 0.1	0.07 ± 0.01	0.4 ± 0.1	0.07 ± 0.01	0.4 ± 0.1	0.09 ± 0.03	0.4 ± 0.1	0.07 ± 0.01	0.6 ± 0.1	0.11 ± 0.01
1:1	0.2 ± 0.2	0.15 ± 0.05	1.0 ± 0.4	0.20 ± 0.03	0.4 ± 0.1	0.09 ± 0.02	0.5 ± 0.1	0.05 ± 0.01	0.3 ± 0.1	0.30 ± 0.02	0.5 ± 0.1	0.10 ± 0.02
1:2	1.7 ± 0.5	0.15 ± 0.03	0.7 ± 0.3	0.17 ± 0.04	0.4 ± 0.1	0.08 ± 0.02	ND	ND	0.6 ± 0.3	0.38 ± 0.06	ND	ND
1:3	1.6 ± 0.4	0.13 ± 0.03	1.0 ± 0.4	0.30 ± 0.04	ND	ND	3.2 ± 1.6	0.20 ± 0.07	0.9 ± 0.3	0.37 ± 0.08	0.4 ± 0.1	0.10 ± 0.01
1:5	ND[b]	ND	ND	ND	0.7 ± 0.2	0.06 ± 0.03	4.6 ± 0.1	0.75 ± 0.07	ND	ND	0.5 ± 0.1	0.07 ± 0.02

[a] Inhibition constants were determined by incubating FBS AChE and FBS AChE−MAb complexes with fasciculin overnight at 22 °C, measuring residual activity, and fitting the data to eq 3. [b] Not determined.

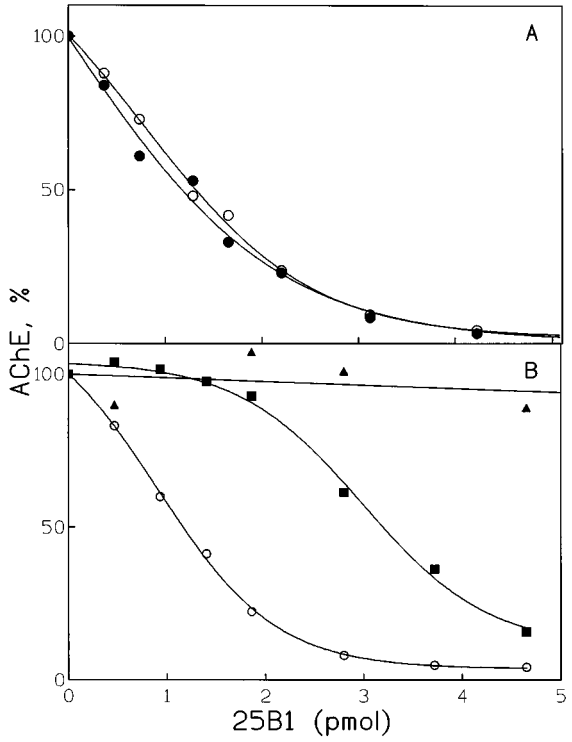

FIGURE 4: Prevention of inhibition of FBS AChE activity by MAb 25B1 in the presence of anti-idiotypic antibodies. A constant amount of buffer (○) or preimmune IgG (500 pmol, ●) (panel A) or anti-idiotypic IgG (100 pmol, ■; 300 pmol, ▲) (panel B) were added to each tube containing 0−5 pmol of MAb 25B1. The mixtures were incubated overnight at 4 °C. One unit of FBS AChE was added to each tube and incubated for 4 h at 22 °C. The enzyme activity in each tube was determined by the Ellman assay (*14*).

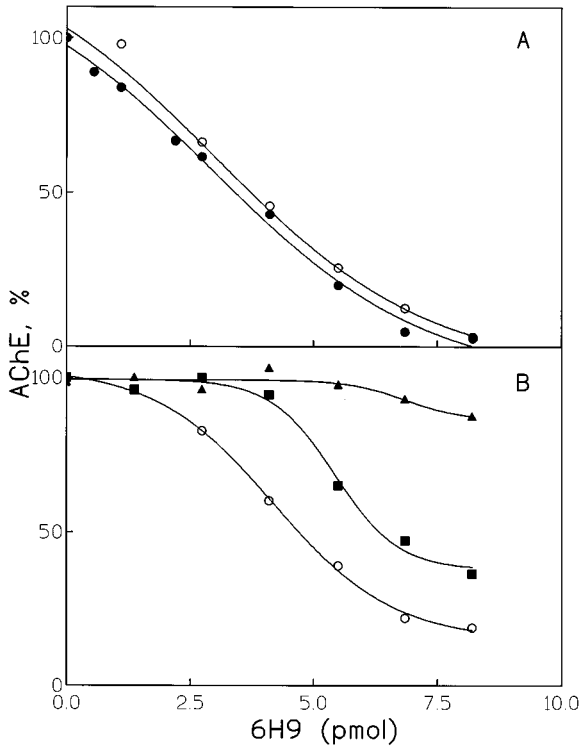

FIGURE 5: Prevention of inhibition of FBS AChE activity by MAb 6H9 in the presence of anti-idiotypic antibodies. A constant amount of buffer (○) or preimmune IgG (500 pmol, ●) (panel A) or anti-idiotypic IgG (100 pmol, ■; 300 pmol, ▲) (panel B) was added to each tube containing 0−10 pmol of MAb 6H9. The mixtures were incubated overnight at 4 °C. One unit of FBS AChE was added to each tube and incubated for 4 h at 22 °C. The enzyme activity in each tube was determined by the Ellman assay (*14*).

only modest changes in K_i for fasciculin. Since fasciculin has a higher affinity for FBS AChE compared to MAbs 13D8 and 2A1, it was able to bind to and inhibit these complexes just as it did the free enzyme.

Characterization of Polyclonal Anti-idiotypic Antibodies to MAbs. We also used the anti-idiotypic antibody approach to identify the MAb combining site. According to the idiotypic network theory of Jerne (*27*), immunization of rabbits with Fab 25B1 and Fab 6H9 should produce antibodies to these MAbs. Indeed ELISA using sera from rabbits immunized with Fab 25B1 and Fab 6H9 showed the presence of specific polyclonal antibodies to MAbs 25B1 and 6H9 (results not shown). The combining sites of these presumed anti-idiotypic antibodies resemble the conformational epitopes on FBS AChE recognized by these MAbs (*28*). As shown in Figure 4, MAb 25B1, upon complexation with its anti-idiotypic antibody, appeared to lose its ability to inhibit the catalytic activity of FBS AChE. By comparing the binding curves for the AChE/MAb interaction in the absence and presence of 100 pmol of IgG containing anti-25B1, the amount of specific anti-idiotypic IgG possessing the ability to neutralize the inhibitory activity of 25B1 was estimated to be 4.25% of the total IgG. The specificity of this reaction was also demonstrated by the inability of preimmune IgG to neutralize the activity of MAb 25B1. Similar results obtained with MAb 6H9 and its anti-idiotypic antibody are shown in Figure 5. The amount of specific anti-idiotypic IgG possessing the ability to neutralize the inhibitory activity of 6H9 was estimated to be 6.5% of the total IgG. These results show that polyclonal anti-idiotypic antibodies raised against MAbs 25B1 and 6H9 neutralized the inhibition of FBS AChE by 25B1 and 6H9, respectively, in a concentration-dependent manner, indicating that these anti-idiotypic antibodies are internal images of the antibody-combining site on FBS AChE.

Further evidence for the generation of an internal image of the peripheral anionic site of FBS AChE on the rabbit anti-idiotypes was obtained by titrating these anti-idiotypic

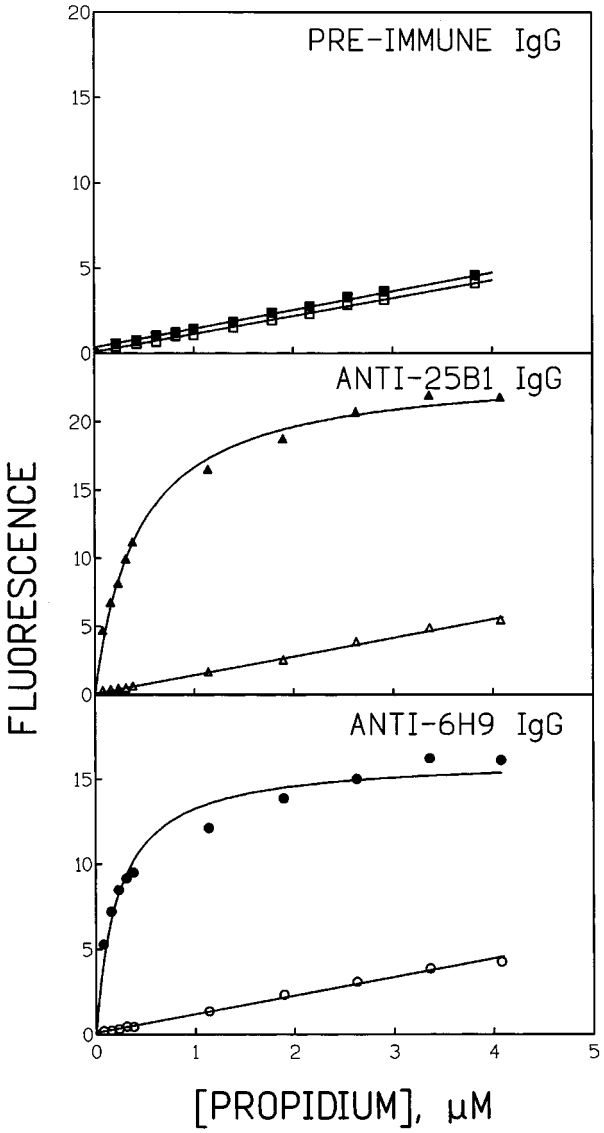

FIGURE 6: Fluorescence intensity of propidium when titrated into solutions of anti-idiotypic antibodies. Separate cuvettes containing 225 μL of preimmune IgG (5.05 μM, ■) or anti-25B1 IgG (23.6 μM, ▲) or anti-6H9 IgG (15.9 μM, ●) in 5 mM Tris·HCl, pH 8.0, and buffer blanks (□, △, ○) were titrated with propidium. The excitation and emission wavelengths were 520 nm and 625 nm, respectively.

antibodies with propidium, a peripheral anionic site ligand (*3*). It was demonstrated that the interaction of propidium, a fluorescent molecule, with *Torpedo* AChE results in a red shift in its absorption spectrum accompanied by fluorescence enhancement (*19*). The value of the dissociation constant (K_D) obtained by this method could be correlated with the inhibition constant (K_i) determined by kinetic studies. As shown in Figure 6, titration of anti-25B1 (23.6 μM) and anti-6H9 (15.9 μM) with propidium in 5 mM Tris·HCl, pH 8.0, resulted in enhancement of propidium fluorescence, which showed saturation as the concentration of propidium was increased. The saturation of fluorescence enhancement occurred at ~1 μM propidium. From calculations described earlier, 23.6 μM anti-25B1 IgG and 15.9 μM anti-6H9 IgG contained ~1 μM specific anti-idiotypic antibodies, respectively. These results show that both anti-idiotypic antibodies bound stoichiometric amounts of propidium, resulting in maximum enhancement of fluorescence, and clearly demonstrate that these antibodies are, in part, internal images of the peripheral anionic site. Scatchard plots of fluorescence titrations (not shown) were linear, indicating an absence of cooperative binding of propidium to the anti-idiotypic antibodies. The dissociation constants, K_D, calculated for anti-25B1 and anti-6H9 from these plots were 2.5 μM and 0.12 μM, respectively. Direct titration of FBS AChE with propidium yielded a K_D of 1.2 μM.

DISCUSSION

Inhibition of cholinesterases by anticholinesterases, such as organophosphates and carbamates, and ligands, such as huperzine A, edrophonium, propidium, tacrine, and ethopropazine, involves one or more of the following interactions: (i) covalent binding to the active site serine; (ii) cation$-\pi$ or $\pi-\pi$ interactions with W86(*84*) and/or the aromatic amino acid residue at position 337(330); (iii) hydrophobic interactions with amino acid residues in the active-site gorge; and (iv) cation$-\pi$ interactions with residues at the peripheral anionic site. On the other hand, peptidic inhibitors such as MAbs and fasciculin selectively interact at the peripheral anionic site of AChE located at the lip of the active site gorge. Recently, several residues involved in peripheral anionic site function were identified by site-directed mutagenesis studies, kinetic studies of inhibition by peripheral anionic site ligands such as propidium and fasciculin, and X-ray crystallographic studies (*9*, *29*−31). These residues are located at the entrance to the active-site gorge and include W286(*279*), Y72(*70*), and Y124(*121*) on one side and D74(*72*) and Y341(*334*) on the other side. The binding of propidium at this site results in inhibition of enzyme activity, which was shown by molecular modeling as well as site-directed mutagenesis studies (*30*, *31*). Molecular modeling studies suggested that binding of propidium at this site blocked the entrance to the gorge, thereby hindering the accessibility of substrate to the active site. However, kinetic data which showed that occupation of the peripheral anionic site by propidium blocked the reactivity of charged but not uncharged substrates toward AChE do not support this conclusion (*32*). Electron paramagnetic resonance studies with spin-labeled organophosphate specifically bound to the active site serine of FBS AChE also revealed that the binding of propidium at the peripheral anionic site did not affect the topography of the active site gorge (*11*).

The peripheral anionic site of AChE is also the site of interaction of fasciculin, a peptide toxin found in the venom of snakes of the mamba family. The interaction of fasciculin at this site results in a selective reversible inhibition of mammalian and *Torpedo* AChE with K_i values in the picomolar range (*24*, *33*). The binding of fasciculin at the peripheral anionic site allosterically affects the orientation of the side chain of W86 located at the base of the gorge (*16*), resulting in a decrease in the acylation rate (*33*). The recently determined X-ray crystal structure of the AChE−fasciculin complex also shows that binding of fasciculin at the peripheral anionic site of AChE sealed the narrow gorge leading to the active site, sterically occluding substrate access to the catalytic site (*25*, *26*). Although these data suggest that the entrance to the catalytic gorge was essentially sealed, kinetic evidence suggests that ligand access to the active-site serine was not completely blocked. This result is

consistent with the 10^3-10^4-fold lower rate constant observed for the binding of *N*-methylacridinium to the AChE−fasciculin complex, compared to AChE (*34*). The extent of this steric blockade depends on the size of the acylation-site ligand (*33*).

Previously we described six inhibitory MAbs generated against FBS AChE which also inhibited the catalytic activity of the enzyme by interacting in the vicinity of the peripheral anionic site. Several of these MAbs, particularly 25B1, 6H9, 4E5, and 5E8, upon binding to FBS AChE were able to inhibit ATC hydrolysis and DFP binding almost completely (>99%) (*10*). It was also shown that binding of these MAbs to FBS AChE resulted in a decrease in the nucleophilicity of the O^{γ} atom of the active site serine to varying degrees, depending on the MAb (*10*). Similarly, the accessibility of this serine to small ligands such as MEPQ and TMB_4 was restricted but not completely blocked in these complexes. These results suggest that the inhibition of FBS AChE was largely due to the binding of these MAbs to antigenic determinant(s) remote from the catalytic site. This result is not surprising since the epitopes of some of the inhibitory antibodies against various AChEs described previously were also located at the peripheral anionic sites of these enzymes (*35*, *36*).

In the present paper, we have further explored the site of interaction of these MAbs on the surface of AChE and how this interaction results in inhibition of enzyme activity. This was investigated by determining the effect of these MAbs on (i) substrate inhibition due to the binding of excess substrate to the peripheral anionic site and (ii) binding of peripheral anionic site ligands, such as propidium and fasciculin. The substrate curves for the complexes of MAbs 4E5, 25B1, and 13D8 were similar to the substrate concentration curve for free enzyme, suggesting that these MAbs did not interfere with the binding of substrate to the peripheral anionic site of FBS AChE. However, for complexes of MAbs 6H9, 5E8, and 2A1, the substrate curves were displaced to the right, suggesting that these MAbs interfered with the binding of substrate to FBS AChE. The accessibility of substrate to the peripheral anionic site in these complexes is restricted but not completely blocked.

The accessibility of the peripheral anionic site to fasciculin in these complexes was determined by measuring residual enzyme activity as a function of fasciculin concentration. The free enzyme, as well as enzyme complexes with the six MAbs, was inhibited by fasciculin. However, unlike mouse AChE, neither the enzyme alone nor the complexes could be inhibited completely even at high fasciculin concentrations. Complexation of FBS AChE with MAbs 25B1, 6H9, 4E5, and 5E8 affected both the K_i for fasciculin, and β, the fraction of residual activity. Site-directed mutagenesis studies with mouse AChE showed that substitution of aromatic residues at the peripheral anionic site, W286(*279*), Y72(*70*), and Y124(*121*), by nonaromatic residues resulted in marked increases in the K_i for fasciculin but no changes in β. Substitutions in the acyl pocket and at position 337 had no effect on inhibition by fasciculin (*24*). However, substitution of W86(*84*) by Y, F, or A did not result in changes in K_i for fasciculin but caused significant increases in β (*16*). Based on these observations and our results presented here, it appears that these MAbs compete for the binding epitopes of fasciculin. These results also suggest that, like fasciculin, binding of MAbs in the vicinity of the peripheral anionic site induced conformational changes in the active site of the enzyme. This proposal was previously made to explain the inhibitory activity of MAb AE-2 although its binding to the peripheral anionic site was not demonstrated (*37*).

The 97−99% decrease in k_{cat} for ATC hydrolysis and slight increases in K_m in the complexes of FBS AChE with MAb 25B1, 6H9, 4E5, and 5E8 compared to free enzyme also suggest that binding of MAbs at the peripheral anionic site allosterically induced conformational changes in the acylation site resulting in decreased hydrolysis of substrate by the enzyme. A similar observation was previously made for the AChE−fasciculin complex (*16*, *33*). Other evidence for MAb-induced changes in conformation of the active site of AChE was recently presented by EPR studies with the FBS AChE−25B1 complex (*11*). Studies with spin-labeled organophosphate specifically bound to the active site serine of FBS AChE revealed that Fab 25B1 bound near the lip of the gorge, resulting in conformational changes leading to narrowing of the gorge. Although the precise location of the MAb combining site of the other MAbs described is not known, it appears that, like fasciculin, they bind near the lip of the gorge, thereby affecting its conformation.

The MAb combining site on FBS AChE was further explored through the use of internal image anti-idiotypic antibodies which have been successfully used as probes for ligand binding sites on receptors (*38*, *39*). The combining site of these anti-idiotypic antibodies not only mimics the structure of the antigen (*40*) but also is able to mimic the functional activity of the antigen (*41*). Indeed polyclonal anti-idiotypic antibodies raised against MAbs 25B1 and 6H9 neutralized the inhibition of FBS AChE by 25B1 and 6H9, respectively, in a concentration-dependent manner, indicating that these anti-idiotypic antibodies are internal images of the antibody combining site on FBS AChE. Titration of anti-25B1 and anti-6H9 with propidium, a peripheral anionic site ligand, showed that both anti-idiotypic antibodies bound stoichiometric amounts of propidium, further demonstrating that these antibodies are, in part, internal images of the peripheral anionic site. The lower dissociation constant of anti-6H9 ($K_D = 0.12\ \mu M$) for propidium compared to anti-25B1 ($K_D = 2.5\ \mu M$) also supports the notion that, although both MAbs 25B1 and 6H9 bind in the vicinity of the peripheral anionic site, the epitopes are slightly different.

In summary, these results demonstrate that inhibitory MAbs against FBS AChE bind at differing but overlapping epitopes located in the vicinity of the peripheral anionic site of the enzyme molecule and can be classified into two groups. The first group includes MAbs 4E5, 25B1, and 13D8, which upon complexation with FBS AChE did not interfere with further binding of substrate to the active site and the peripheral anionic site. These MAbs form multimeric complexes with FBS AChE, and these complexes inhibit the hydrolysis of ATC, a charged substrate, as well as IPA, a neutral substrate (*10*). The second group includes MAbs 6H9, 5E8, and 2A1, which upon binding to FBS AChE affected the binding of substrate to the active site as well as the peripheral anionic site. These MAbs formed a single discrete complex with FBS AChE, and these complexes inhibited the hydrolysis of ATC, but marginally affected or stimulated the hydrolysis of IPA. Like fasciculin, the binding

of these MAbs in the vicinity of the peripheral anionic site at the rim of the gorge allosterically affects the orientation of W86(*84*) which stabilizes the quaternary group of the substrate, resulting in inhibition of enzyme activity. Although these MAbs appear to affect the occlusion of substrates and inhibitors to the active site gorge, the oxime TMB_4 was still able to reach the gorge and dissociate DFP from the active site serine. The FBS AChE−MAb 6H9 complex was more restrictive to the displacement of the organophosphoryl-bound moiety by TMB_4 as compared to the FBS AChE−MAb 25B1 complex. These results suggest that either the complexes undergo conformational changes to allow the entry of the oxime through the active site gorge or there is an alternate portal for the entry of oxime, such as the proposed back door region (*42*, *43*). Since these MAbs appear to affect the orientation of W86 which is located near the proposed back door region, they can be used as tools to further explore this region.

ACKNOWLEDGMENT

We thank Mary Kay Gentry for providing monoclonal and anti-idiotypic antibodies for use in these studies and help with preparation of the manuscript. We thank D. Scott Frazier, Ann M. G. Redman, and James Fedorko for their expert technical assistance. We also thank Dr. Zoran Radić for his advice on fasciculin binding experiments.

REFERENCES

1. Hobbiger, F. (1976) *Handb. Exp. Pharmak. 42*, 487−581.
2. Quinn, D. M. (1987) *Chem. Rev. 87*, 955−975.
3. Taylor, P., and Lappi, S. (1975) *Biochemistry 14*, 1989−1997.
4. Mooser, G., and Sigman, D. S. (1974) *Biochemistry 13*, 2299−2307.
5. Sussman, J. L., Harel, M., Frolow, F., Oefner, C., Goldman, A., Toker, L., and Silman, I. (1991) *Science 253*, 872−879.
6. Shinitzky, M., Dudai, Y., and Silman, I. (1973) *FEBS Lett. 30*, 125−128.
7. Goeldner, M. P., and Hirth, C. G. (1980) *Proc. Natl. Acad. Sci. U.S.A. 77*, 6439−6442.
8. Weise, C., Kreienkamp, H.-J., Raba, R., Pedak, A., Aaviksaar, A., and Hucho, F. (1990) *EMBO J. 9*, 3885−3888.
9. Harel, M., Schalk, I., Ehret-Sabatier, L., Bouet, F., Goeldner, M., Hirth, C., Axelsen, P. H., Silman, I., and Sussman, J. L. (1993) *Proc. Natl. Acad. Sci. U.S.A. 90*, 9031−9035.
10. Gentry, M. K., Moorad, D. R., Hur, R. S., Saxena, A., Ashani, Y., and Doctor, B. P. (1995) *J. Neurochem. 64*, 842−849.
11. Grubić, Z., Štalc, A., Šentjurc, M., Pećar, S., Gentry, M. K., and Doctor, B. P. (1995) *Biochim. Biophys. Acta 1249*, 155−160.
12. Massoulié, J., Sussman, J. L., Doctor, B. P., Soreq, H., Velan, B., Cygler, M., Rotundo, R., Shafferman, A., Silman, I., and Taylor, P. (1992) in *Multidisciplinary Approaches to Cholinesterase Functions* (Shafferman, A., and Velan, B., Eds.) pp 285−288, Plenum Press, New York.
13. De La Hoz, D., Doctor, B. P., Ralston, J. M., Rush, R. S., and Wolfe, A. D. (1986) *Life Sci. 39*, 195−199.
14. Ellman, G. L., Courtney, K. D., Andres, V., Jr., and Featherstone, R. M. (1961) *Biochem. Pharmacol. 7*, 88−95.
15. Haldane, J. B. S. (1930) in *The Enzymes*, Longmans-Green, London.
16. Radić, Z., Quinn, D. M., Vellom, D. C., Camp, S., and Taylor, P. (1995) *J. Biol Chem. 270*, 20391−20399.
17. Ackermann, W. W., and Potter, V. R. (1949) *Proc. Soc. Exp. Biol. Med. 72*, 1−9.
18. Mooser, G., Schulman, H., and Sigman, D. (1972) *Biochemistry 11*, 1595−1602.
19. Taylor, P., Lwebuga-Mukasa, J., Lappi, S., and Rademacher, J. (1974) *Mol. Pharmacol. 10*, 703−708.
20. Ashani, Y., Gentry, M. K., and Doctor, B. P. (1990) *Biochemistry 29*, 2456−2463.
21. Radić, Z., Reiner, E., and Taylor, P. (1990) *Mol. Pharmacol. 39*, 98−104.
22. Marchot, P., Khelif, A., Ji, Y. H., Mansuelle, P., and Bougis, P. E. (1993) *J. Biol. Chem. 268*, 12458−12467.
23. Durán, R., Cerveñansky, C., Dajas, F., and Tipton, K. F. (1994) *Biochim. Biophys. Acta 1201*, 381−388.
24. Radić, Z., Durán, R., Vellom, D. C., Li, Y., Cerveñansky, C., and Taylor, P. (1994) *J. Biol. Chem. 269*, 11233−11239.
25. Bourne, Y., Taylor, P., and Marchot, P. (1995) *Cell 83*, 503−512.
26. Harel, M., Kleywegt, G. J., Ravelli, R. B. G., Silman, I., and Sussman, J. L. (1995) *Structure 3*, 1355−1366.
27. Jerne, N. K. (1974) *Ann. Inst. Pasteur 125C*, 373−389.
28. Doctor, B. P., Gentry, M. K., Wu, S.-J., Ashani, Y., and De La Hoz, D. M. (1991) in *Cholinesterases: Structure, Function, Mechanism, Genetics, and Cell Biology* (Massoulié, J., Bacou, F., Barnard, E., Chatonnet, A., Doctor, B. P., and Quinn, D. M., Eds.) pp 37−41, American Chemical Society, Washington, D.C.
29. Shafferman, A., Kronman, C., Flashner, Y., Leitner, M., Grosfeld, H., Ordentlich, A., Gozes, Y., Cohen, S., Ariel, N., Barak, D., Harel, M., Silman, I., Sussman, J. L., and Velan, B. (1992) *J. Biol. Chem. 267*, 17640−17648.
30. Barak, D., Kronman, C., Ordentlich, A., Ariel, N., Bromberg, A., Marcus, D., Lazar, A., Velan, B., and Shafferman, A. (1994) *J. Biol. Chem. 269*, 6296−6305.
31. Barak, D., Ordentlich, A., Bromberg, A., Kronman, C., Marcus, D., Lazar, A., Ariel, N., Velan, B., and Shafferman, A. (1995) *Biochemistry 34*, 15444−15452.
32. Berman, H. A., Leonard, K., and Nowak, M. W. (1991) in *Cholinesterases: Structure, Function, Mechanism, Genetics, and Cell Biology* (Massoulié, J., Bacou, F., Barnard, E., Chatonnet, A., Doctor, B. P., and Quinn, D. M., Eds.) pp 229−234, American Chemical Society, Washington, D.C.
33. Eastman, J., Wilson, E. J., Cerveñansky, C., and Rosenberry, T. L. (1995) *J. Biol. Chem. 270*, 19694−19701.
34. Rosenberry, T. L., Rabl, C.-R., and Neumann, E. (1996) *Biochemistry 35*, 685−690.
35. Brimijoin, S., Mintz, K. P., and Pendergast, F. G. (1985) *Mol. Pharmacol. 28*, 539−545.
36. Remy, M. H., Frobert, Y., and Grassi, J. (1995) *Eur. J. Biochem. 231*, 651−658.
37. Wolfe, A. D., Chiang, P. K., Doctor, B. P., Fryar, N., Rhee, J. P., and Saeed, M. (1993) *Mol. Pharmacol. 44*, 1152−1157.
38. Pain, D., Kanwar, Y. S., and Blobel, G. (1988) *Nature 331*, 232−237.
39. Vaux, D., Tooze, J., and Fuller, S. (1990) *Nature 345*, 495−502.
40. Garcia, K. C., Desiderio, S. V., Ronco, P. M., Verroust, P. J., and Amzel, L. M. (1992) *Science 257*, 528−531.
41. Taub, R., and Greene, M. I. (1992) *Biochemistry 31*, 7431−7435.
42. Ripoll, D. R., Faerman, C. H., Axelsen, P. H., Silman, I., and Sussman, J. L. (1993) *Proc. Natl. Acad. Sci. U.S.A. 90*, 9031−9035.
43. Axelsen, P. H., Harel, M., Silman, I., and Sussman, J. L. (1994) *Protein Sci. 3*, 188−197.

BI972061O